Vol 16 No 11, November 2007
1009-1963/2007/16(11)/3359-11

Chinese Physics

© 2007 Chin. Phys. Soc.
and IOP Publishing Ltd

First-principle studies of the geometries and electronic properties of $Cu_mSi_n(2 \leq m+n \leq 7)$ clusters

Liu Xia(刘　霞), Zhao Gao-Feng(赵高峰)†, Guo Ling-Ju(郭令举),
Wang Xian-Wei(王献伟), Zhang Jun(张　俊), Jing Qun(井　群), and Luo You-Hua(罗有华)

Institute of Theoretical Physics, School of Physics and Electronics, Henan University, Kaifeng 475004, *China*

(Received 20 December 2006; revised manuscript received 9 May 2007)

The equilibrium geometries and electronic properties of Cu_mSi_n ($2 \leq m+n \leq 7$) clusters have been studied by using density functional theory at the B3LYP/6-311+G (d) level. Our results indicate that the structure of $CuSi_n$ (n <6) keeps the frame of the corresponding Si_n cluster unchanged, while for Cu_nSi clusters, the rectangular pyramid structure of Cu_4Si is shown to be a building block in many structures of larger Cu_nSi clusters. The growth patterns of Cu_mSi_n clusters become more complicated as the number of Cu atoms increases. Both the binding energies and the fragmentation energies indicate that the Si–Si bond is stronger than the Cu–Si bond, and the latter is stronger than the Cu–Cu bond. Combining the fragmentation energies in the process $Cu_mSi_n \rightarrow Cu+Cu_{m-1}Si_n$ and the second-order difference $\Delta_2 E(m)$ against the number of Cu atoms of Cu_mSi_n, we conclude that Cu_mSi_n clusters with even number of Cu atoms have higher stabilities than those with odd m. According to frontier orbital analyses, there exists a mixed ionic and covalent bonding picture between Cu and Si atoms, and the Cu d orbitals contribute little to the Cu–Si bonding. For a certain cluster size ($m+n$ = 3, 4, 5, 6, 7), the energy gaps of the most stable Cu_mSi_n clusters show odd–even oscillation with changing m, the clusters with odd m exhibit stronger chemical reactivity than those with even m.

Keywords: Cu_mSi_n clusters, density functional theory, structures and properties
PACC: 3640B, 3640C, 7115M

1. Introduction

Nowadays, the microelectronic devices are becoming miniaturized, and it is expected that the spatial extension of electronic elements will soon approach the size of clusters. Thus, it is of fundamental importance to explore the structures and electronic properties of clusters. Substantial efforts have focused on elucidating the geometric, electronic, and energetic properties of pure silicon clusters due to its potential applications in the field of electronic materials.[1−5]

Meanwhile, binary clusters have been also substantially investigated.[6−11] In the last two decades, several experimental studies have dealt with metal-doped silicon clusters. Using laser vaporization experiment, Kishi *et al* produced Si_nNa_m ($1 \leq n \leq 14$, $1 \leq m \leq 5$) binary clusters.[12] Beck [13] used a laser vaporization supersonic expansion technique to investigate small $MeSi_n$(Me = Cu, Cr, Mo, and W) clusters; he reported that such clusters turned out to be more stable toward photofragmetation than the corresponding bare Si_n clusters. Specifically, for $CuSi_n$ clusters, Beck[13] pointed out that there was a pronounced abundance maximum at $CuSi_{10}$ in the range of $6 \leq n \leq 12$. Consequently, using cavity ringdown laser absorption spectroscopy and time-of-flight mass spectroscopy, Scherer *et al*, who identified several series of smaller Cu_mSi_n clusters ($m \leq 3$, $n \leq 9$),[14] complemented Beck's investigation.

Stimulated by these experimental results, several computational investigations have been performed on the geometric, electronic, and energetic properties of metal-doped silicon clusters,[15−19] including $CrSi_n$ (n = 8–17),[15] $ReSi_n$(n = 1–12),[16] $TaSi_n$(n = 1–13),[17] $ZrSi_n$(n = 1–16),[18] Si_nM(M = Ti,Zr,Hf).[19] The principal problem in studying metal-doped silicon clusters is the comprehension of the modifications of properties compared with the case of bare silicon clusters. With noble-silicon clusters, Xiao *et al* have performed several computational studies on the geometric and electronic properties of $CuSi_n$ by using a hybrid density functional technique (B3LYP).[20−24] They pointed out that the Si_n frameworks in most stable isomers of $CuSi_n$ adopt the geometries of the

†Corresponding author. E-mail: zgf@henu.edu.cn

ground state or low-lying isomers of Si_n or Si_{n+1}, with Cu at various adsorption or substitutional sites.

However, Xiao *et al*'s investigations mainly focused on the clusters containing one Cu atom. What about the geometric and energetic properties of small Cu–Si binary clusters containing many Cu atoms? Wu and Hagelberg have investigated the geometries and energetic properties of Me_mSi_{7-m} (Me = Cu and Li, $m \leq 6$) clusters in terms of density functional theory (DFT) employing a plane wave basis.[25] According to their investigations, pentagonal ground state structures derived from the D_{5h} equilibrium geometries of both Si_7 and Cu_7 clusters were obtained for Cu_mSi_{7-m} with $m < 6$. However, the investigations on smaller clusters have, to our knowledge, scarcely been reported, and calculations of Cu_mSi_n ($2 \leq m+n \leq 6$, $m \geq 2$) clusters have not been systemically studied. In the present paper, geometric and energetic properties of Cu_mSi_n ($2 \leq m+n \leq 7$) are systematically studied by the first-principle method based on the DFT. The study of Cu–Si clusters could furnish a better understanding in the interaction between Si and Cu atoms, and could contribute to the answer of the topical question of the degree to which various metal elements can be solvated in finite semiconductor structures.

This paper is organized as follows: Section 2 gives a brief description of the computational method. Section 3 presents the main results and discussions. Main conclusions are summarized in Section 4.

2. Computational method

In this paper, all the calculations for Cu_mSi_n ($2 \leq m+n \leq 7$) clusters are performed with the B3LYP[26] hybrid density functional method and the 6-311+G (d) basis set in the Gaussian 03[27] package. In order to test the quality of the B3LYP/6-311+G (d) scheme for the description of Cu–Si binary clusters, we have calculated some properties of the Si and Cu atoms and Cu_2, Si_2, CuSi dimers. As shown in Table 1, the calculated bond lengths, binding energies per atom, vibrational frequencies, ionization potentials, and electron affinities for Si and Cu atoms and their dimers are in fairly good agreement with the available experimental data.[28−34] Therefore, we have confidence to use the same basis set throughout the whole calculation. The calculation convergence criterion for energy is set to 1×10^{-5} eV.

Table 1. The bond length (R_e), binding energy per atom (E_b), vibrational frequency (ω_e), ionization potential (IP), and electron affinity (EA) of Cu, Si, Cu_2, Si_2 and CuSi at DFT/B3LYP/6-311+G(d) level.

cluster		R_e	E_b/eV	ω_e/cm^{-1}	IP/eV	EA/eV
Si	B3LYP/6-311+G(d)				8.109	1.441
	Expt.				8.15[28]	1.385[29]
Si_2	B3LYP/6-311+G(d)	2.280	1.532	485.8	8.601	2.046
	Expt.	2.246[30]	1.604[30]	509±10[31]	7.921[32]	2.176±0.002[31]
Cu	B3LYP/6-311+G(d)				8.033	1.212
	Expt.[33]				7.724	1.235±0.005
Cu_2	B3LYP/6-311+G(d)	2.277	0.902	239.772	7.997	0.729
	Expt.[33]	2.22	1.04±0.01	265	7.904	0.836±0.006
CuSi	B3LYP/6-311+G(d)	2.249	1.019	323.933		
	Expt.[34]	2.28	1.125	320		

We firstly calculate the geometrical structures of pure Cu and Si clusters so that these pure clusters might be regarded as the reference of the initial geometries of Cu–Si binary clusters. For Si-rich clusters, we try to start the geometry optimization of Cu_mSi_n clusters in the frame of the corresponding Si_n clusters, in which Cu atoms are located on Si atoms or bridged over two atoms or capped on several atoms or substituted for Si atoms. While for Cu-rich clusters, similar methods are also used. All optimizations are carried out without symmetry constraints (C_1 symmetry group). The stabilities of Cu_mSi_n clusters are examined by evaluating the harmonic frequencies. For each of these clusters, all the computed frequencies have been confirmed to be real. In the case of an imaginary frequency, the relaxation along the corresponding unstable normal coordinate is carried out until a true local minimum is reached. Therefore, the energies of

the geometric structures for these clusters are indeed at their local minima on the potential energy surfaces. We have started with a spin-singlet configuration for the even-electron systems and a spin-doublet configuration for the odd-electron systems until the energy minimum is reached. For each stable structure, binding energies per atom (E_b), fragmentation energies (E_f), vertical ionization potentials (VIP) and energy gaps (E_g) of Cu_mSi_n clusters are then calculated and discussed. Furthermore, the geometries and energetic properties for the pure Cu_n, Si_n ($n = 1$–7) clusters are also presented for comparison.

3. Results and discussions

The optimized geometries of the Cu_mSi_n clusters, including the Cu_n and Si_n structures, are shown in Figs.1–3. We adopt the labels m, n, y, where m and n denote the numbers of Cu and Si atoms in the Cu_mSi_n cluster, respectively, while $y(= a, b\cdots)$ denotes the rank of the order of energy. For instance, a and b indicate the most stable and the next stable structures, respectively.

3.1. Cu_mSi_n($m = 0, 1, 2 \le m + n \le 7$ and $n = 0, 1, 2 \le m + n \le 7$)

For Cu_mSi_n (m = 0, 1, 2 $\le m + n \le$ 7 and n = 0, 1, 2 $\le m + n \le$ 7) clusters, the lowest energy structures and their isomers are shown in Fig.1. The ground state of all the clusters examined is doublet except for Cu_2Si, Cu_4Si and Cu_6Si whose ground state is singlet. The ground state structures of Cu_4Si and Cu_5Si possess C_{4v} symmetry and those of $CuSi_2$, $CuSi_3$ and Cu_2Si are all of C_{2v} symmetry, while the symmetry of $CuSi_4$, $CuSi_5$, $CuSi_6$ and Cu_3Si reduces to C_s. For the $CuSi_n$ clusters, the structures of the most stable isomers retain the framework of the corresponding Si_n except $CuSi_6$. This means that the Si–Si bond predominates over the Cu–Si one. Our results obtained for the structural and the electronic properties of the lowest energy isomers are similar to those in Ref.[24] in DFT/B3LYP calculations except for $CuSi_3$. Our calculation shows that in Fig.1 1.3.a is more stable than 1.3.b, being higher in energy than the latter by 0.181 eV; however, the result in Ref.[24] is opposite to this.

Due to the very weak s–d electron hybridization, Cu_n clusters tend to form three-dimensional (3D) structures, that is, the lowest energy structures of Cu_n ($n \le$6) are planar structures, while that of Cu_7 cluster is 3D with a pentagon bipyramid geometry. This result is in good agreement with previous theoretical work.[35] For the Cu_nSi ($n \ge$2) clusters, only Cu_2Si shows the planar structure. The ground state structure of Cu_3Si is a bent rhombus. The lowest energy structure of Cu_4Si is a rectangular pyramid, which is a building block in many structures of larger Cu_nSi clusters. For example, Cu_5Si, Cu_6Si can be described as Cu atom capping on various adsorption sites of Cu_4Si.

3.2. Cu_mSi_n($n = 2, 2 \le m \le 5$ and $n = 3$, $2 \le m \le 4$)

The geometries of the Cu_mSi_2, Cu_mSi_3 clusters are shown in Fig.2. It is found that the ground state is a singlet for m = 2, 4, while it is a doublet for m = 3, 5. The most stable structure of Cu_2Si_2 2.2.a is a bent rhombus (C_{2v}) including four equal Cu–Si bonds. An initial structure with two Cu atoms substituting two connected Si atoms of Si_4 relaxes to 2.2.b, which is 0.547 eV higher in energy than 2.2.a. For Cu_3Si_2, 3.2.a is a trigonal bipyramid with C_s symmetry, resembling the Si_5 species. While an isomer with three Cu atoms replacing three Si atoms at the equatorial sites of Si_5 relaxes to a deformed rectangular pyramid 3.2.b, being higher in energy than 3.2.a by 0.251 eV. Cu_4Si_2 has three low-lying isomers, in which 4.2.a is a C_{2v} face-capped trigonal bipyramid. 4.2.b and 4.2.c have the structures of an edge-capped trigonal bipyramid and a rectangular bipyramid, being higher in energy than 4.2.a by 0.409 eV and 0.621 eV, respectively.

As to Cu_5Si_2, similar to the results in Ref.[25], a structure derived from the D_{5h} prototype defines the lowest energy state of Cu_5Si_2 5.2.a (C_{2v}); whereas 5.2.b is a bi-capped trigonal bipyramid, being higher in energy than 5.2.a only by 0.062 eV. We also obtain another two similar face-capped rectangular bipyramid structures 5.2.c and 5.2.d, which are 0.139 eV and 0.981 eV higher in energy than 5.2.a, respectively.

For Cu_mSi_3 (m = 2, 3, 4,) clusters, the ground state structure of Cu_2Si_3 2.3.a is irregular with C_{2v} symmetry, two Cu atoms and two Si atoms form a bent Cu_2Si_2 rhombus and one Si atom is located above this rhombus. Cu_2Si_3 2.3.b is a trapezoidal planar structure, which is 0.272 eV higher in energy than 2.3.a, and 2.3.c is a side-adsorbed structure with one Si atom attaching to a Cu_2Si_2 framework, being higher in energy than 2.3.a by 0.714 eV. The equilibrium struc-

ture of Cu_3Si_3 3.3.a (C_1) has a face-adsorbed geometry with one Cu atom on the face of the Cu_2Si_2 rectangular pyramid. The structures of 3.3.b and 3.3.c adopt a rectangular bipyramid and a face-capped trigonal bipyramid, which are higher in energy than 3.3.a by 0.139 eV and 0.380 eV, respectively.

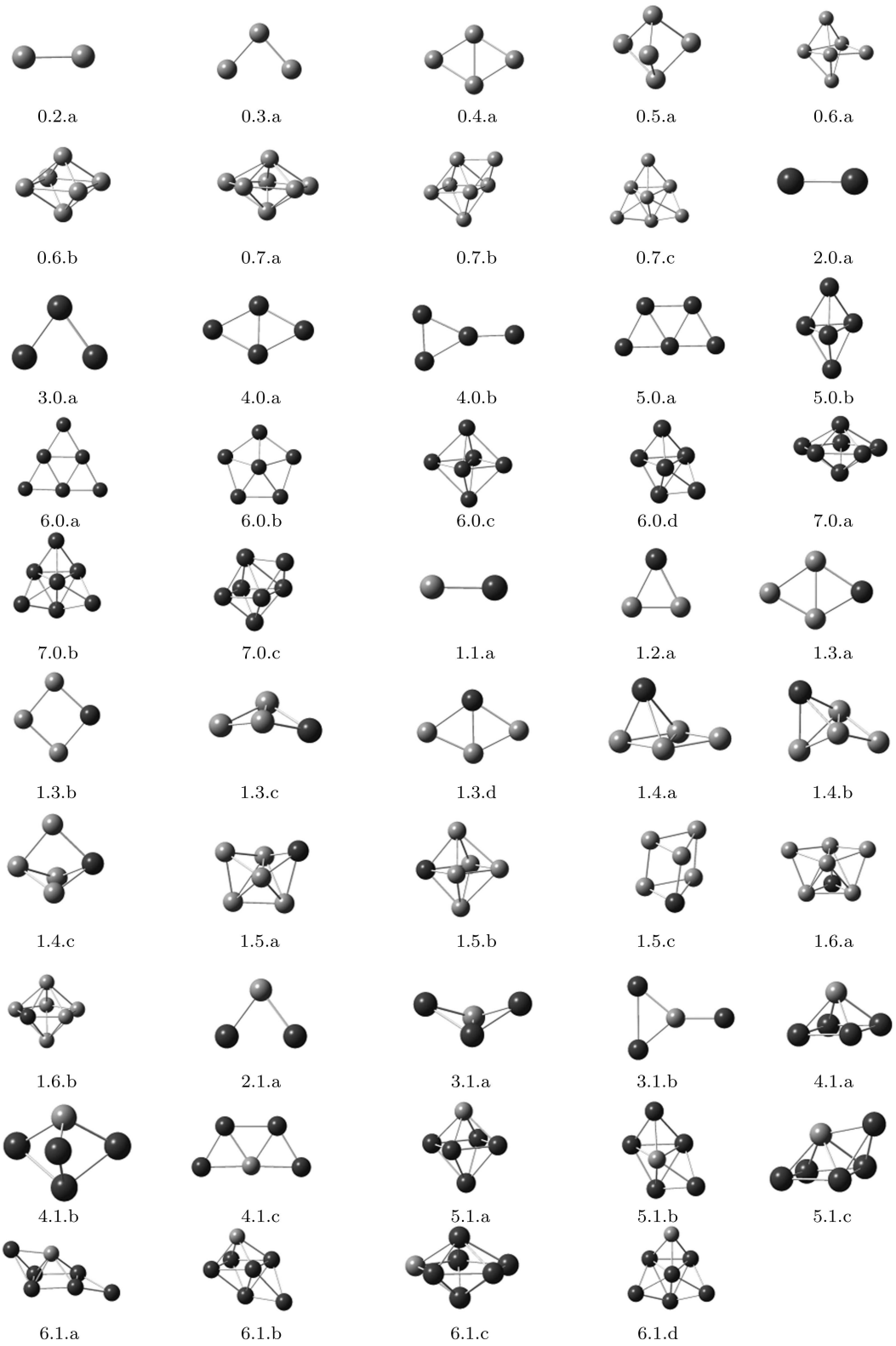


Fig.1. Optimized geometries of Cu_mSi_n (m = 0, 1, $2 \le m+n \le 7$ and n = 0, 1, $2 \le m+n \le 7$) clusters at the B3LYP/6-311+G (d) level. The dark and grey spheres represent Cu and Si atoms, respectively.

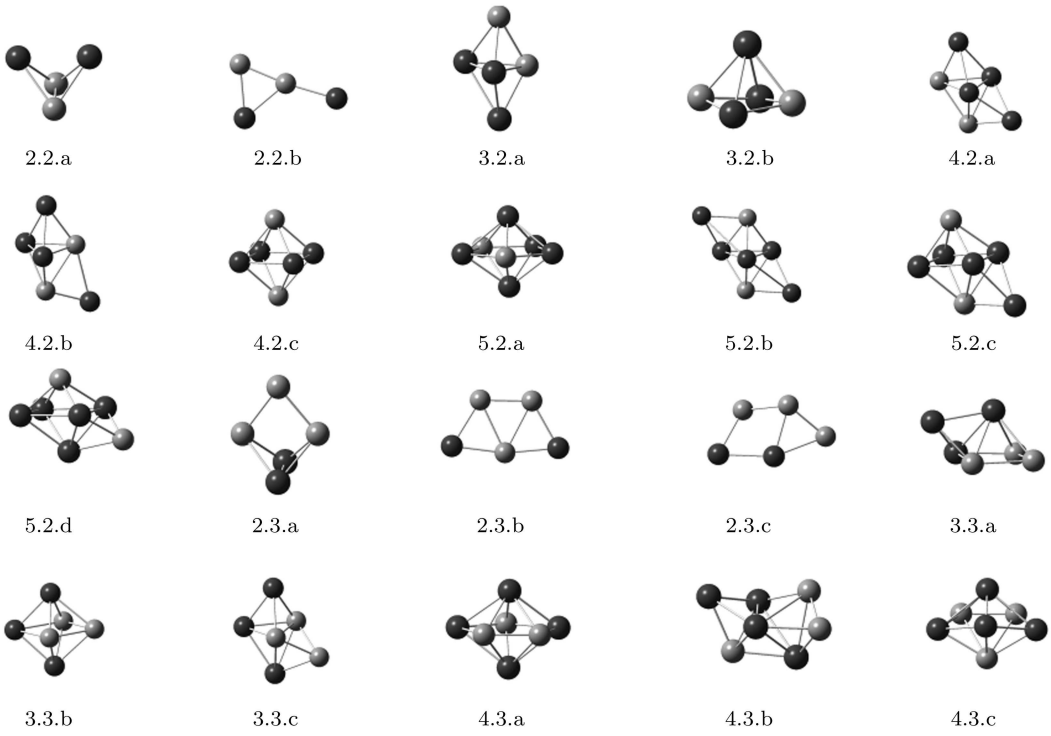


Fig.2. Optimized geometries of Cu_mSi_n ($n = 2$, $2 \leq m \leq 5$ and $n = 3$, $2 \leq m \leq 4$) clusters at the B3LYP/6-311+G (d) level. The dark and grey spheres represent Cu and Si atoms, respectively.

For Cu_4Si_3, our calculations agree well with the results in Ref.[25]. Either 4.3.a or 4.3.c can be described as a distorted pentagonal bipyramid, the latter is higher in energy than the former by 0.104 eV, while 4.3.b is a bi-capped trigonal bipyramid, being higher in energy than 4.3.a only by 0.029 eV.

3.3. Cu_2Si_4, Cu_3Si_4 and Cu_2Si_5

The ground states of Cu_2Si_4 and Cu_2Si_5 considered here are both singlet and that of Cu_3Si_4 is doublet. As shown in Fig.3, Cu_2Si_4 2.4.a is a deformed triangular prism (C_2) with two Cu atoms at different sides; 2.4.b and 2.4.c are near-degenerate, being higher in energy than 2.4.a by 0.089 eV and 0.138 eV, respectively.

Similar to Ref.[25], the ground state of Cu_3Si_4 3.4.a (C_2) is characterized by three Cu atoms substituted for three connected Si atoms at equatorial sites of Si_7. An isomer 3.4.b originating from four Si atoms replacing four Cu atoms of Cu_7 7.0.c turns out to be higher in energy than 3.4.a by 0.042 eV. Wu and Hagelberg[25] calculated a substitutional structure with three disconnected Cu atoms at the equatorial sites of Si_7, while our results show that this structure is unstable. Additionally, an initial substitutional structure with three Cu atoms at the outside sites of Si_7 0.7.c relaxes to 3.4.c, which is 0.159 eV higher in energy than 3.4.a.

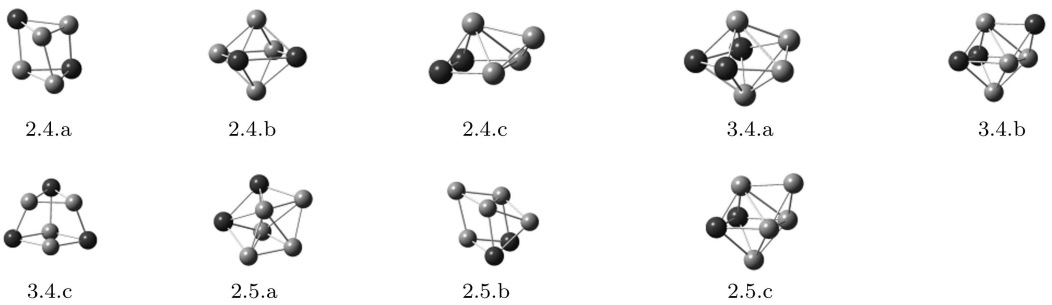


Fig.3. Optimized geometries of Cu_2Si_4, Cu_3Si_4 and Cu_2Si_5 clusters at the B3LYP/6-311+G (d) level. The dark and grey spheres represent Cu and Si atoms, respectively.

Similar to Cu_3Si_4, the equilibrium structure of Cu_2Si_5 2.5.a and 2.5.b calculated are in agreement with the results in Ref.[25]. The third lowest structure 2.5.c originates from two Cu atoms substituted for two Si atoms at the equatorial sites of Si_7 0.7.b and is 0.980 eV higher in energy than 2.5.a.

3.4. Growth patterns of Cu_mSi_n clusters

The growth patterns of Cu_mSi_n clusters could be figured out from Figs.1–3 (only look at the ground state structures denoted in a). The ground state structures of $CuSi_n (n < 6)$ can be derived from those of the Si_n clusters by capping one Cu atom on various surface sites of Si_n, which is similar to the growth pattern of $NaSi_n$ clusters.[12] While for Cu_nSi clusters, the rectangular pyramid structure of Cu_4Si is a building block in many structures of larger Cu_nSi clusters.

In another perspective consideration, for Cu_mSi_n $(m + n = 4)$ clusters, all the Si_4, Cu_4 and $CuSi_3$ structures are planar rhombus while the structures of Cu_2Si_2 and Cu_3Si prefer to be the bent rhombus. As to the Cu_mSi_n $(m + n = 5, 6)$ clusters, owing to the considerable difference between the 3D structures of Si_5 and Si_6 and the planar structures of Cu_5 and Cu_6, the growth patterns of Cu_mSi_n $(m+n = 5, 6)$ clusters become more complicated. Whereas for $Cu_mSi_n (m+n = 7)$ clusters, we obtain pentagonal bipyramid structures in the most stable clusters except for Cu_6Si.

In Ref.[24], it was shown that charge transfers from Cu to Si. In our calculation, there is also charge transfer from Cu to Si atom owing to the larger electronegativity of the Si atom than that of the Cu atom. This result has been reflected in the structures of the Cu_mSi_n clusters described above. For example, in Cu_2Si_2 cluster, the bond distance of Cu_2 subunit (0.2575 nm) is distinctly closer to that of Cu_2 cation (0.2448 nm) than that of the neutral molecule (0.2278 nm). While in Cu_2Si_5, two Cu atoms form a dimer with a distance of 0.2604 nm, and this value is close to that of Cu_2^+. A similar charge transfer is found in $NaSi_n$ and $TaSi_n (n = 1–11)$.[12,17] A charge-transfer proceeding in the opposite direction, from Si_n to transition metal (TM), was recorded for $CrSi_n$.[15]

3.5. Electronic and bonding properties of Cu_mSi_n clusters

We now discuss the size-dependent physical properties of these clusters. The binding energies per atom (E_b), the fragmentation energies (E_f) with respect to $Cu_mSi_n \rightarrow Si + Cu_mSi_{n-1}$ or $Cu + Cu_{m-1}Si_n$, the vertical ionization potentials (VIP) for Cu_mSi_n and the corresponding values of pure Si_n and Cu_n clusters are shown in Table 2. We expect that these data may be helpful for experimental studies in the future.

The binding energies per atom (E_b) for the most stable isomers of $CuSi_n$, Cu_nSi, Cu_{n+1} and Si_{n+1} (n = 1–6) with respect to isolated atoms are presented in Table 2, and their size dependences are shown in Fig.4. For all the clusters except CuSi, the stabilities of Si_{n+1}, $CuSi_n$, Cu_nSi and Cu_{n+1} are in the order of $Si_{n+1} > CuSi_n > Cu_nSi > Cu_{n+1}$. Therefore, the Si–Si bond is stronger than the Cu–Si bond and the latter is stronger than the Cu–Cu bond.

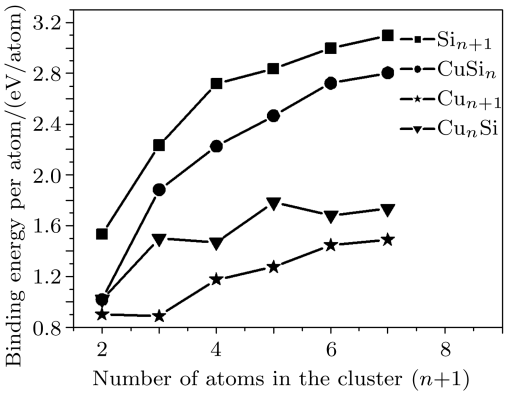


Fig.4. Binding energies per atom (E_b) for the most stable isomers of $CuSi_n$ and Cu_nSi ($n \leq 7$) and Si_{n+1}, Cu_{n+1} (n = 1–6) clusters at the B3LYP/6-311+G (d) level.

As shown in Table 2, E_b of Cu_mSi_n (m = 1, 2, 3, 4, 5) clusters increases with increasing number of Si atoms. Thus, the clusters can continue to gain energy during the growth process. In another perspective experiment, E_b of Si_2 is larger than that of Cu_2 and E_b of CuSi lies in between the E_b's of Cu_2 and Si_2 clusters (Table 1). Thus, we may expect that the E_b of the Cu–Si binary clusters tends to increase with increasing number of Si atoms. Indeed, as shown in Fig.5, E_b's of Cu_mSi_n ($m + n$ = 4, 5, 6, 7) clusters increase with increasing number of Si atoms. E_b's of Cu_mSi_n clusters lie between those of corresponding pure Cu_{m+n} and Si_{m+n} clusters. It thus can be shown that the Si-rich clusters are more stable than the Cu-rich ones for the clusters with the same size.

Table 2. The binding energy per atom (E_b), fragmentation energy (E_f), vertical ionization potential (VIP) and (HOMO–LUMO) gap (E_g) for the Cu_mSi_n ($2 \le m+n \le 7$) clusters.

cluster	E_b/eV	fragmentation process	E_f/eV	fragmentation process	E_f/eV	VIP/eV	E_g/eV
Si_2	1.532	Si+Si	3.064			8.601	1.644
Si_3	2.234	Si+Si_2	3.638			8.222	2.382
Si_4	2.718	Si+Si_3	4.171			8.137	2.423
Si_5	2.836	Si+Si_4	3.307			8.164	3.171
Si_6	2.998	Si+Si_5	3.811			7.937	3.252
Si_7	3.099	Si+Si_6	3.703			8.038	3.161
Cu_2	0.902			Cu+Cu	1.804	7.997	3.238
Cu_3	0.887			Cu+Cu_2	0.857	6.041	1.309
Cu_4	1.177			Cu+Cu_3	2.046	6.703	1.934
Cu_5	1.275			Cu+Cu_4	1.667	6.336	1.371
Cu_6	1.446			Cu+Cu_5	2.302	7.226	3.170
Cu_7	1.490			Cu+Cu_6	1.752	6.056	1.295
CuSi	1.019	Si+Cu	2.037	Cu+Si	2.037	7.243	1.616
$CuSi_2$	1.884	Si+CuSi	3.615	Cu+Si_2	2.589	7.436	1.497
$CuSi_3$	2.225	Si+$CuSi_2$	3.247	Cu+Si_3	2.198	7.950	1.643
$CuSi_4$	2.465	Si+$CuSi_3$	3.427	Cu+Si_4	1.453	7.107	1.664
$CuSi_5$	2.721	Si+$CuSi_4$	4.002	Cu+Si_5	2.148	7.619	1.930
$CuSi_6$	2.804	Si+$CuSi_5$	3.299	Cu+Si_6	1.636	6.909	1.606
Cu_2Si	1.498	Si+Cu_2	2.481	Cu+CuSi	2.247	7.333	2.060
Cu_3Si	1.470	Si+Cu_3	3.700	Cu+Cu_2Si	2.077	6.727	1.810
Cu_4Si	1.786	Si+Cu_4	4.222	Cu+Cu_3Si	2.567	7.457	3.378
Cu_5Si	1.681	Si+Cu_5	3.710	Cu+Cu_4Si	1.155	5.857	1.561
Cu_6Si	1.735	Si+Cu_6	3.466	Cu+Cu_5Si	2.058	6.532	2.602
Cu_2Si_2	2.060	Si+Cu_2Si	3.955	Cu+$CuSi_2$	2.588	6.966	2.703
Cu_2Si_3	2.234	Si+Cu_2Si_2	2.932	Cu+$CuSi_3$	2.272	7.598	2.784
Cu_2Si_4	2.422	Si+Cu_2Si_3	3.359	Cu+$CuSi_4$	2.204	7.425	2.203
Cu_2Si_5	2.692	Si+Cu_2Si_4	4.313	Cu+$CuSi_5$	2.516	7.473	3.052
Cu_3Si_2	1.895	Si+Cu_3Si	3.112	Cu+Cu_2Si_2	1.234	6.288	1.577
Cu_3Si_3	2.116	Si+Cu_3Si_2	3.225	Cu+Cu_2Si_3	1.526	6.653	1.476
Cu_3Si_4	2.382	Si+Cu_3Si_3	3.977	Cu+Cu_2Si_4	2.144	7.030	1.482
Cu_4Si_2	1.920	Si+Cu_4Si	2.593	Cu+Cu_3Si_2	2.048	6.784	2.257
Cu_4Si_3	2.140	Si+Cu_4Si_2	3.461	Cu+Cu_3Si_3	2.285	6.586	2.175
Cu_5Si_2	1.888	Si+Cu_5Si	3.135	Cu+Cu_4Si_2	1.697	6.317	1.584

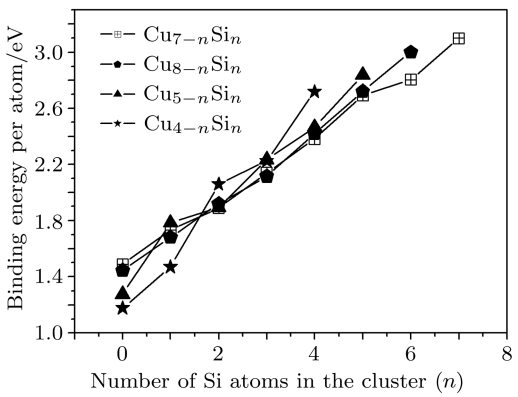


Fig.5. Binding energy per atom (E_b) for Cu_mSi_n ($m+n$ = 4, 5, 6, 7) clusters versus the number of Si atoms n for the most stable structures.

Studying the fragmentation energies (E_f) is also an appropriate way for comparing the local stabilities of different sizes of Cu_mSi_n clusters and comparing the relative strengths of Si–Si, Cu–Si and Cu–Cu interactions. As shown in Table 2, the E_f's with respect to the process of Cu_mSi_n →Si+Cu_mSi_{n-1} are higher than those of the Cu_mSi_n →Cu+$Cu_{m-1}Si_n$. This result shows that the bonding strengths are arranged in the order of Si–Si>Cu–Si>Cu–Cu, following the same hierarchy established by the E_b's.

Considering the bonding strength order Si–Si>Cu–Si, it is much easier to dissociate a Cu atom than a Si atom from the Cu_mSi_n clusters. In the fol-

lowing, we only discuss the E_f's of Cu_mSi_n ($n = 1, 2, 3, 4, 5$) clusters in the process $Cu_mSi_n \rightarrow Cu+Cu_{m-1}Si_n$. As seen from Fig.6, all of the five curves show odd–even oscillation, and their maxima are found at $m = 2, 4, 6$. We thus predict that Cu_mSi_n ($n = 1, 2, 3, 4, 5$) clusters with even Cu atoms have higher stability than the clusters with odd m.

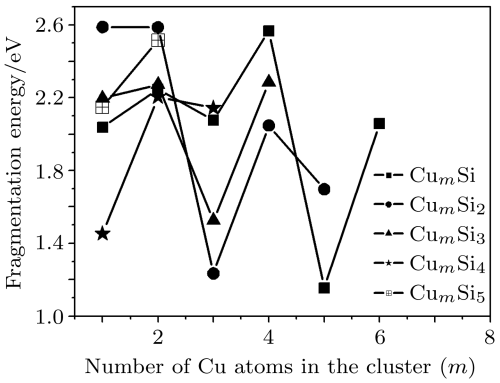


Fig.6. Fragmentation energy (E_f) for the Cu_mSi_n ($n = 1, 2, 3, 4, 5$) clusters versus the number of Cu atoms m for the most stable structures.

In cluster physics, the second-order difference of cluster energies $\Delta_2 E\ (n)$ is a sensitive quantity that reflects the relative stability of clusters. Figure 7 shows the second-order difference of cluster energies $\Delta_2 E(m)$ against the number of Cu atoms, that is $\Delta_2 E\ (m, n) = E(m+1, n) + E(m-1, n) - 2E(m, n)$.

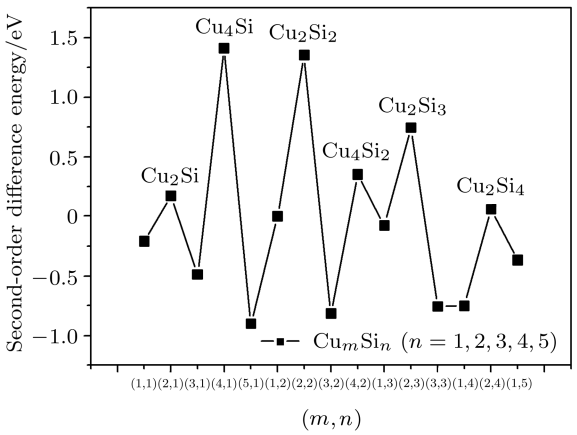


Fig.7. The second–order differences of cluster energies for Cu_mSi_n($n = 1, 2, 3, 4, 5$) clusters.

Maxima are found at Cu_2Si, Cu_4Si, Cu_2Si_2, Cu_4Si_2, Cu_2Si_3 and Cu_2Si_4, indicating that these clusters possess higher stabilities, which are consistent with the results of the E_f's shown in Fig.6.

We now illustrate the bonding properties for Cu_mSi_n clusters. Table 2 shows that the VIPs of $CuSi_n$ clusters are lower than that of the pure Si_n clusters. This reduction reflects the change in the orbital ionization. As seen from Fig.8, the highest occupied molecular orbital (HOMO) of $CuSi_n$ corresponds to the lowest unoccupied molecular orbital (LUMO) of Si_n except that of $CuSi_6$. This result is in agreement with the growth patterns of $CuSi_n$ clusters. For example, the LUMO of Si_4 is composed of the p orbitals on the two Si atoms of the long diagonal and is weakly antibonding between them. When one Cu atom caps the Si_4 rhombus, the p orbitals still exist on the long diagonal of Si atoms, and there is a significant s and p characters on the Cu atom. For $CuSi_5$, its HOMO is similar to the LUMO of Si_5 with a little modification due to the presence of Cu, and the d orbitals of Cu exhibit only a small degree of hybridization with the s, p orbitals of Si. While for $CuSi_6$, its HOMO is much different from the LUMO of Si_6, but is similar to the HOMO of Si_7. This is consistent with the fact that the ground state structure of $CuSi_6$ 1.6.a originates from one Cu atom substituted for one Si atom at the apical site of Si_7.

As seen from Fig.8, the d orbitals of Cu are much more localized, exhibiting only a small degree of hybridization with the orbitals of Si, and there is a strong hybridization between the s and p orbitals of Cu and those of Si atoms. Thus, we may understand that there exists a mixed ionic and covalent bonding picture between Cu and Si atoms, and the Cu d orbitals contribute little to the Cu–Si bonding. For further analysis, from the HOMOs of the $CuSi_5$, $CuSi_6$, Cu_2Si_5 and Cu_5Si_2, one can notice that the HOMO states are mainly localized around Si atoms. But there are also some distributions of HOMO states around Cu atoms and antibonding interactions between Cu atoms in the HOMOs of Cu_2Si_5 and Cu_5Si_2. All these results further confirm the bonding strength order of Si–Si, Cu–Si and Cu–Cu given above.

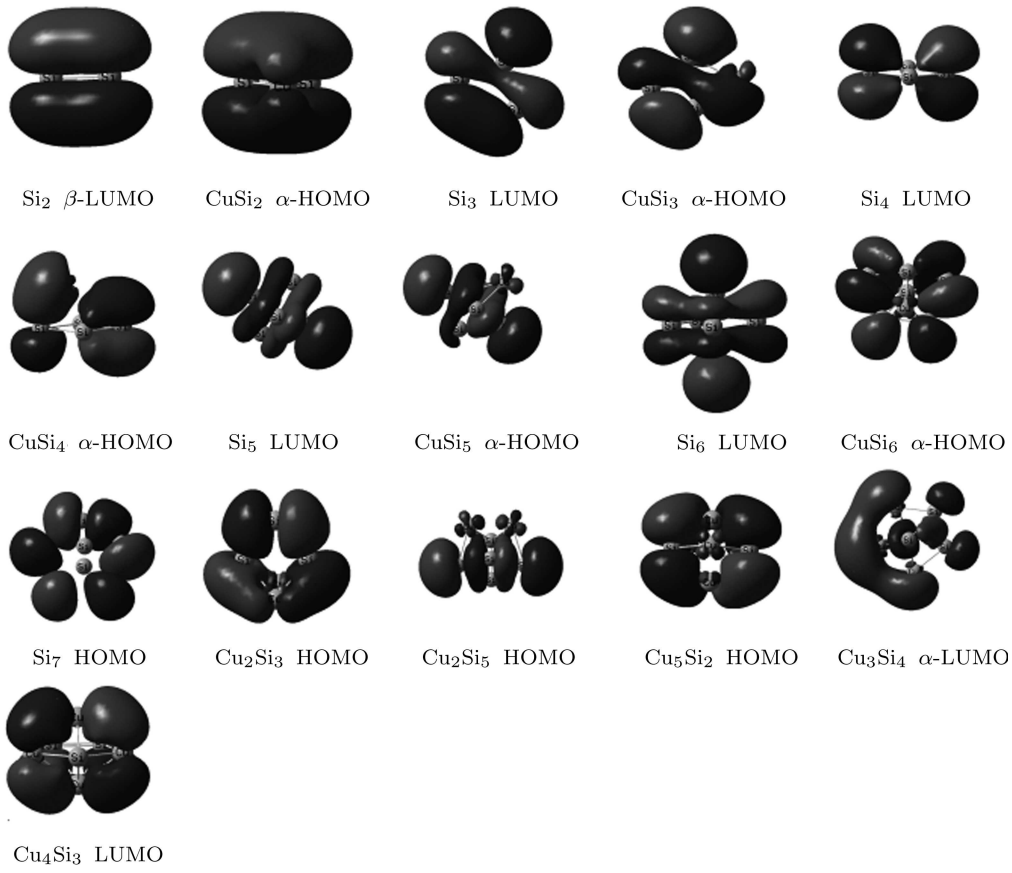


Fig.8. Contour maps of the HOMOs and LUMOs of the selected Cu_mSi_n and Si_n clusters.

3.6. HOMO–LUMO Gap

Semiconducting characters of semiconductive material silicon and the TM-doped silicon clusters can be reflected from the energy gap (E_g) between the HOMO and the LUMO. The E_g's we obtained for pure Cu_n clusters agree well with those determined by Wang *et al*[35] using a B3LYP/lanl2DZ calculations except for Cu_5 and Cu_7. As seen from Table 2, E_g's of $CuSi_n$ are distinctly lower than those of Si_n clusters. The similar trend is also found in other TM-silicon clusters.[17] This means that the metallic characteristics of $CuSi_n$ clusters are enhanced. Detailed analyses of the electronic levels show that the HOMO and LUMO are mainly composed of Cu s-states mixed with Si s, p-states. Therefore, it is the sp-hybridization that is responsible for the reduction of energy gap with addition of Cu. In contrast, the E_g's of Cu_n are increased when one Si is doped into the Cu_n clusters except Cu_2Si and Cu_6Si whose energy gaps are lower than those of the corresponding Cu_2 and Cu_6, respectively.

As shown in Table 2, the E_g's of pure Si_n clusters are larger than those of the Cu_n clusters except Cu_2. Thus, we may expect that the E_g's of Cu_mSi_n clusters tend to decrease as the system changes from pure Si_n to pure Cu_n. The E_g's of Cu_mSi_n ($m+n=3$, 4, 5, 6, 7) clusters are shown in Fig.9, in which we can see

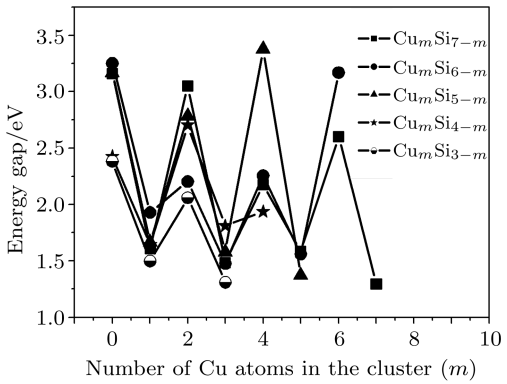


Fig.9. Energy gaps (E_g) for Cu_mSi_n ($m+n=3$, 4, 5, 6, 7) clusters versus the number of Cu atoms m for the most stable structures.

our calculations for Cu_mSi_{7-m} clusters agree well with those in Ref.[25]. All the four curves show the odd–even oscillation behaviour, the E_g's of the clusters with odd Cu atoms are much smaller than those of the clusters with even Cu atoms. It is well known that the HOMO–LUMO gap reflects the relative chemical reactivity of clusters. Our results indicate that the clusters with odd Cu atoms exhibit stronger chemical reactivity than the clusters with even Cu atoms.

4. Conclusions

In this paper, we have calculated the geometries and electronic properties of Si_n, Cu_n, and Cu_mSi_n ($2 \leq m+n \leq 7$) clusters at the DFT/B3LYP/ 6-311+G(d) level. All the calculated results are summarized as follows:

(1) The ground states examined for Cu_mSi_n clusters with even m are all singlet while those of the clusters with odd m are all doublet.

(2) The structure of $CuSi_n$ ($n < 6$) retains the framework of the corresponding Si_n cluster. This means that the Si–Si bond predominates over the Cu–Si one. While for Cu_nSi clusters, the rectangular pyramid structure of Cu_4Si is shown to be a building block in many structures of larger Cu_nSi clusters. The growth patterns of Cu_mSi_n clusters become more complicated as the number of Cu atoms increases.

(3) The calculated energetic properties show that the bonding strengths can be arranged in the order of Si–Si>Cu–Si>Cu–Cu. The E_b's of Cu_mSi_n ($m+n$ = 4, 5, 6, 7) clusters tend to increase with increasing number of Si atoms. Both the E_f's of Cu_mSi_n (n = 1, 2, 3, 4, 5) and the Δ_2E (m) show that the Cu_mSi_n clusters with even number of Cu atoms have higher stabilities than those with odd m. According to frontier orbitals analyses, the HOMO of $CuSi_n$ ($n < 6$) corresponds to the LUMO of Si_n with a little modification due to the presence of Cu. While for $CuSi_6$, its HOMO corresponds to the LUMO of Si_7. This result is consistent with the growth patterns of $CuSi_n$ clusters. There exists a mixed ionic and covalent bonding picture between Cu and Si atoms and the Cu d orbitals contribute little to the Cu–Si bonding.

(4) The HOMO–LUMO gaps (E_g) of $CuSi_n$ clusters decrease obviously as compared with the pure Si_n clusters. While for the Cu_mSi_n ($m+n$ = 3, 4, 5, 6, 7) clusters, theE_g's of the clusters with odd number of Cu atoms are much smaller than those of the clusters with even number of Cu atoms, which indicates that the clusters with odd m exhibit stronger chemical reactivity than the clusters with even m.

References

[1] Wang J, Zi J, Zhang K M and Xie X D 1993 *Acta Phys. Sin.* **42** 423 (in Chinese)
[2] Liu Y Z and Luo C L 2004 *Acta Phys. Sin.* **53** 592 (in Chinese)
[3] Yoo S and Zeng X C 2003 *J. Chem. Phys.* **119** 1442
[4] Wang J and Wang S Q 2003 *Acta Phys. Sin.* **52** 2854 (in Chinese)
[5] Yang J C, Xu W G and Xiao W S 2005 *J. Mol. Struct.* (THEOCHEM) **719** 89
[6] Li C B, Li M K, Yin D, Liu F Q and Fan X J 2005 *Chin. Phys.* **14** 2287
[7] Chen Z Z and Wang C Y 2006 *Chin. Phys.* **15** 604
[8] Chen L J 2006 *Chin. Phys.* **15** 798
[9] Fang F, Jiang G and Wang H Y 2006 *Acta Phys. Sin.* **55** 2241 (in Chinese)
[10] Wang H Y, Li X B, Tang Y J, Chen X H, Wang C Y and Zhu Z H 2005 *Acta Phys. Sin.* **54** 3566 (in Chinese)
[11] Li E L, Yang C J, Chen G C, Wang X W and Ma D M 2005 *Acta Phys. Sin.* **54** 4117 (in Chinese)
[12] Kishi R, Iwata S, Nakajima A and Kayo K 1997 *J. Chem. Phys.* **107** 3056
[13] Beck S M 1989 *J. Chem. Phys.* **90** 6306
[14] Scherer J J, Paul J B, Collier C P and Saykally R J 1995 *J. Chem. Phys.* **102** 5190
[15] Kawamura H, Kumar V and Kawazoe Y 2004 *Phys. Rev.* B **70** 245433
[16] Han J G, Ren Z Y and Lu B Z 2004 *J. Phys. Chem.* A **108** 5100
[17] Guo P, Ren Z Y, Wang F, Bian J, Han J G and Wang G H 2004 *J. Chem. Phys.* **121** 12265
[18] Wang J and Han J G 2005 *J. Chem. Phys.* **123** 064306
[19] Kawamura H, Kumar V and Kawazoe Y 2005 *Phys. Rev.* B **71** 075432
[20] Xiao C and Hagelberg F 2000 *J. Mol. Struct.* (THEOCHEM) **529** 241
[21] Xiao C, Hagelberg F, Ovcharenko I and Lester W A Jr 2001 *J. Mol. Struct.* (THEOCHEM) **549** 181
[22] Ovcharenko I V, Lester W A Jr, Xiao C and Hagelberg F 2001 *J. Chem. Phys.* **114** 9028
[23] Xiao C, Hagelberg F and Lester W A Jr 2002 *Phys. Rev.* B **66** 075425
[24] Xiao C, Abraham A, Quinn R, Hagelberg F and Lester W A Jr 2002 *J. Phys. Chem.* A **106** 11380

[25] Wu J H and Hagelberg F 2006 *J. Phys. Chem.* A **110** 5901
[26] Becke A D 1993 *J. Chem. Phys.* **98** 1372
[27] Frisch M J, Trucks G W, Schlegel H B *et al* Gaussian 03, 2004 Revision C.02 (Wallingford CT: Gaussian, Inc.)
[28] Moore C E 1971 *Analysis of Optical Spectra* NSRDES-NBS 34 (Washington, DC: National Bureau of Standards)
[29] Hotop H and Lineberger W C 1975 *J. Phys. Chem.* Ref.Data **4** 539
[30] Huber K P and Herzberg G 1979 *Constants of Diatomic Molecules* (New York: Van Nostrand Reinhold)
[31] Kitsopoulos T N, Chick C J, Zhao Y and Neumark D M 1991 *J. Chem. Phys.* **95** 1441
[32] Marijnissen A and ter Meulen J J 1996 *Chem. Phys. Lett.* **263** 803
[33] Calaminici P, Koster A M, Russo N and Salahub D R 1996 *J. Chem. Phys.* **105** 9546
[34] Scherer J J, Paul J B, Collier C P and Saykally R J 1995 *J. Chem. Phys.* **103** 113
[35] Wang H Y, Li C Y, Tang Y J and Zhu Z H 2004 *Chin. Phys.* **13** 677